Dielectric characteristic of nanocrystalline Na0.5K0.5NbO3 ceramic green body

Laijun Liu, Huiqing Fang, Liang Fang, Hichem Dammak, Maï Pham-Thi

J Electroceram (2012) 28:144–148
DOI 10.1007/s10832-012-9695-6

Dielectric characteristic of nanocrystalline $Na_{0.5}K_{0.5}NbO_3$ ceramic green body

Laijun Liu · Huiqing Fan · Liang Fang · Hichem Dammak · Mai Pham-Thi

Received: 30 November 2010 / Accepted: 17 February 2012 / Published online: 29 February 2012

Abstract Dielectric spectroscopy was applied to porous nanocrystalline $Na_{0.5}K_{0.5}NbO_3$ (NKN) ceramic green body, wherein influences of percolation effect and water adsorption at pore surface of the ceramic green body on dielectric response were examined over wide temperature (150 to 450 K) and frequency (100 Hz to 1 MHz) ranges. Dielectric permittivity of the ceramic green body is about 2–3 orders of magnitude higher than that of pure NKN powder or NKN ceramic. Furthermore, the high dielectric permittivity and high humidity sensitivity of the ceramic green body can appear again with aging a period of time in air. The data from this investigation make potential applications for NKN as a giant dielectric material or a humidity sensing material.

L. Liu (✉) · L. Fang
Key laboratory of Nonferrous Materials and New Processing Technology, Ministry of Education,
Guilin University of Technology,
Guilin 541004, China
e-mail: ljliu2@163.com

L. Liu · H. Fan
State Key Laboratory of Solidification Processing,
School of Materials Science and Engineering,
Northwestern Polytechnical University,
Xi'an 710072, China

L. Liu · H. Dammak
Laboratoire Structures, Propriétés et Modélisation des Solides,
Ecole Centrale Paris, CNRS-UMR8580,
Grande voie des Vignes,
92295 Châtenay-Malabry Cedex, France

M. Pham-Thi
THALES Research & Technology France,
Campus Polytechnique, 1 Avenue Augustin Fresne,
91767 Palaiseau Cedex, France

Keywords Dielectric relaxation · Porous · Percolation theory · $Na_{0.5}K_{0.5}NbO_3$

1 Introduction

Sodium potassium niobate, $Na_{0.5}K_{0.5}NbO_3$ (NKN), is a ferroelectric material with perovskite structure which has important practical applications in piezoelectric devices and infrared pyroelectric detectors, using its excellent piezoelectric and pyroelectric properties as lead-free electroceramics [1–5]. However, low dielectric permittivity (ε= 200 ~ 500) restricts the possible applications as capacitor and filter.

Generally, high dielectric capacitors are made of thin layers of ceramic material placed between conductive plates [6]. IBLC (internal barrier layer capacitors) [7] and MLCC (multi-layer ceramic capacitors) [8] are some of the most efficient geometries for attaining high-density charge storage. Unfortunately, it is very difficult for NKN ceramics to form electrical heterogeneous structure because the concentrations of oxygen vacancy in grain and grain boundary are not possible to control during sintering and cooling process. Furthermore, residual stress degrades the mechanical and electrical properties of ceramic phase for multilayer ceramic capacitors (MLCC) duo to the phase stability of pure NKN is as high as 1140°C.

Percolation theory was initially developed to describe several abrupt transitions commonly found in transport phenomena. It is well known that metal-insulator composite demonstrates a metal-insulator transition with increasing metal concentration [9, 10], identical to the Mott transition around its critical temperature [11]. The metal-insulator transition is usually characterized by an abrupt discontinuity in the real part of conductivity. The effective dielectric permittivity

of a mixture exhibits an increase in the neighborhood of the percolation threshold and is much larger than those of the components [12–15]. There are many conducting particles isolated by insulation layers or insulating particles isolated by conducting layers to form much many micro-capacitors at the percolation threshold point [13–15]. Thus, a heterogeneous system in the neighborhood of the percolation threshold could become a capacitor with an excellent characteristic of charge storage.

In our recent work, we fabricated nanocrystalline NKN ceramic green body, a mixture of three phases, namely NKN nanoparticle, nanopore and water molecule. Temperature dependence of dielectric properties of the green body was investigated. Non-Debye relaxations present in wide frequency and temperature ranges based on interface polarization and percolation effects.

2 Experimental

Carbonates and oxides Na_2CO_3 (PROLABO, 99.9%), $K_2CO_3{\cdot}1.5H_2O$ (MERCK, 99.995%) and Nb_2O_5 (INTERCHIM, 99.5%) were used as starting materials. Retsch mill (PM 100) was used for mechanical alloying to fabricate NKN powder. Perovskite NKN powder was obtained after milling 450 rpm for 2 h and then calcined at 850°C for 2.5 h. The calcined powder was pressed into discs uniaxially of 10 mm in diameter and 2 mm in thickness under 300 MPa and then pressed under 650 MPa with a cool isostatic pressing method.

Crystal phase of the NKN powder was determined using X-ray diffractometry (XRD; SIEMENS D5000) in θ–2θ mode with graphite monochromatized Cu $K\alpha$ radiation. Average grain size the NKN powder was calculated from the full width at half maximum (FWHM) of diffraction lines according to Scherrer's relation:

$$d = \frac{K\lambda}{B\cos\theta} \tag{1}$$

where d is the grain diameter, λ the X-ray wavelength, θ the diffraction angle, B the FWHM of the diffraction peak, and K the Scherrer constant. Porosity characteristic of the green body was analyzed by using nitrogen adsorption equipment (Autosorb-Quantachrome NOVA 1200). And the green body was outgassed for 2 h at 550 K before that analysis. Microstructural morphology of the green body fracture was observed by scanning electron microscope (SEM, JSM-6380LV). To understand water desorption of the green body, thermogravimetric analysis (TGA) and differential scanning calorimetric (DSC) analysis is performed using a TGA/SDTA851 analyzer (Mettler Toledo) in the temperature range of 300–550 K in an air atmosphere at heating rate of 10 K/min. Both sides of the fresh ceramic green body were printed Ag electrodes. Electrical properties measurement was taken with an applied voltage of 500 mV over the frequency range 100 Hz–5 MHz from 150 K to 450 K at heating rate of 3 K/min with an impedance analyzer (Agilent 4294A).

3 Results and discussion

XRD pattern of the NKN nanopowder prepared by mechanical alloying method is shown in Fig. 1. The powder has a pure perovskite structure, and displays a typical orthorhombic symmetry at room temperature. Although the structure of NKN is orthorhombic at room temperature, the perovskite type ABO_3 subcell possesses a monoclinic symmetry, with lattice parameters $a_m=c_m > b_m$ while b_m is perpendicular to the a_mc_m plane and the angle *beta* is a little bit more than 90°. Therefore, the peaks can be indexed based on according to monoclinic symmetry (ICSD collection code: 038004). Average crystallite size of the powder prepared in this study is about 70 nm which deduces from the XRD pattern by Scherer equation with subtraction of the equipment widening. Figure 2 shows SEM micrograph of the green body. The green body presents a porous structure, constituted by agglomerated particles and pores. Nano-size particle leads to the formation of ultra-small pores with a diameter of tens of nanometers. Such ultra-small pore is part of the structure of the porous NKN ceramic green body. The porosity value of the green body is 21%, measured by the nitrogen adsorption method of Brunauer-Emmett-Teller (BET).

In fact, the green body can be considered as a mixture of three phases, namely solid phase, liquid phase and gaseous phase. The solid phase is formed by the nanocrystalline NKN particle. The liquid phase is represented by water molecule and the gaseous phase by air. Similar to porous silica glasses [16–19], water can be easily adsorbed by

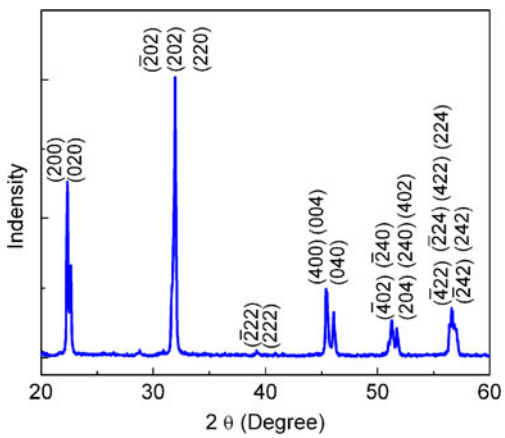

Fig. 1 XRD pattern of $Na_{0.5}K_{0.5}NbO_3$ nanopowder

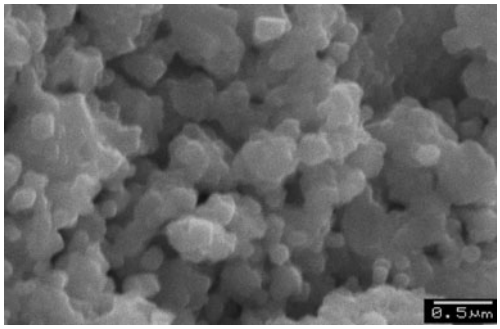

Fig. 2 SEM image of nanocrystalline $Na_{0.5}K_{0.5}NbO_3$ ceramic green body

nanocrystalline particle because many defects exist on the surface of nanoparticle, furthermore, K^+ and Na^+ ions have strong hygroscopic in NKN. Therefore, a lot of water molecules will be absorbed by the green body.

TGA and DSC results of the green body were displayed in Fig. 3. As seen in the figure, the weight loss of the green body terminates at about 500 K. The weight loss from room temperature to 500 K can be ascribed to the evaporation of absorbed water, while endothermic peaks in the DSC curve could correspond to the state change of absorbed water.

The dielectric response induced by water adsorption will be found to be very sensitive to the amount water molecules on adsorptive layer of the particle surface [18]. Spectra of the dielectric permittivity and loss associated with the relaxation induced by water molecules of the adsorptive layer for the green body versus frequency and temperature are displayed in Fig. 4(a) and (b). The complex dielectric behavior can be described in terms of three distributed relaxation processes.

The first relaxation process is observed in the low temperature region from 200 K to 350 K. There is a part of this process which most likely shifts to the high frequency limit that is out of the frequency range. In this process, the weight loss of the green body is very slight near 330 K but an

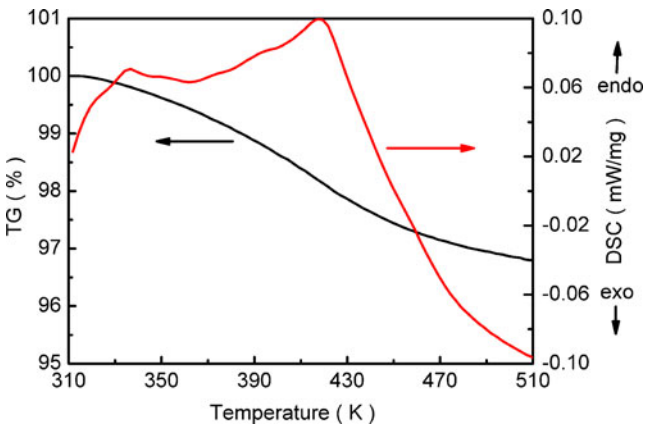

Fig. 3 TGA and DSC results of nanocrystalline $Na_{0.5}K_{0.5}NbO_3$ ceramic green body

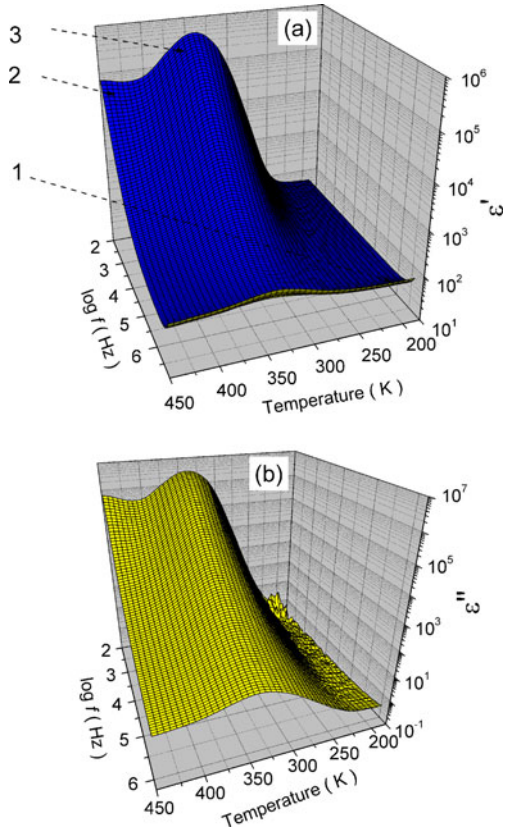

Fig. 4 Three-dimensional plot of the complex dielectric permittivity real ε' (**a**) and imaginary part ε'' (**b**) versus frequency and temperature for the green body

endothermic peak can be detected in the DSC curve (Fig. 3). It was shown that the hindered dynamics of the water molecules located within the pores reflect the interaction of the absorptive layer with the inner surfaces of the green body. The temperature dependence of dielectric properties (Fig. 4(a) and (b) of the first process correlates with that of pure ice [20]. However, unlike the Debye relaxation of pure ice, the relaxation in the green body demonstrates a non-Debye dependence, which can be connected to variance of the morphology of pores and the interaction of water molecules with the pores surface [16]. A similar dielectric relaxation behavior in silica-water systems at low water content was observed and ascribed to reorientation of water molecules in ice-like structure [17–19]. Therefore, the first process should arise from the same relaxation mechanism.

The second relaxation process has a part of saddle-like shape in the temperature range of 400–450 K. The green body shows an increase in dielectric permittivity (Fig. 4(a)) and dielectric loss (Fig. 4(b)) in the low-frequency limit. This relaxation process looks likes an interface polarization process, thus causing build-up of macroscopic charge separation or space charge. However, NKN is an insulator at this temperature region, and the space charge relaxation presents above 700 K [21, 22]. Therefore, this relaxation process

does not associate with space charge relaxation. According to a model based on the idea of Macedo and Litovitz [23], this relaxation process occurs as a result of the ice structure defects motion.

The third relaxation process presents in the low-frequency region and the temperature interval 250–400 K. The amplitude of this process essentially decreases with the increase of frequency. Furthermore, the maximum of the dielectric permittivity occurs at the temperature of about 340 K which is almost frequency independent. A strong endothermic peak and an acute weight loss can be detected in this temperature region (Fig. 3). Finally, the low-frequency ac-conductivity σ_{ac} demonstrates an *S*-shape dependency with the increase of temperature (Fig. 5), which is typical for percolation [17–19]. So this dielectric relaxation process results from percolation of the apparent dipole moment excitation within the developed fractal structure of the connected pores [17, 18] This excitation is associated with the self-diffusion of the charge carriers in the porous net.

The temperature dependence of ac-conductivity has three distinct stages in the third relaxation process, named pre-percolation range, percolation range and post-percolation range. The activation energy (E_a) of the percolation for the green body has been estimated on the basis of an Arrhenius form of relation:

$$\sigma_{ac} = A \exp\left(-\frac{E_a}{k_B T}\right) \tag{2}$$

where A is a constant, σ_{ac} is the ac-conductivity, T is the temperature and k_B is Boltzmann constant. E_a value can be obtained from the slope of ln σ_{ac} against 1,000/T plot, shown in Fig. 6. The activation energies of the three distinct stages are 0.083 eV, 0.454 eV and 0.296 eV, respectively.

The activation energies of conductivity are lower in the pre- and post-percolation range than that in the percolation, which are in the order of normal electrolyte conductance [24]. It is considered that the lower activation energy corresponds to a more open structure. Water molecules in cluster

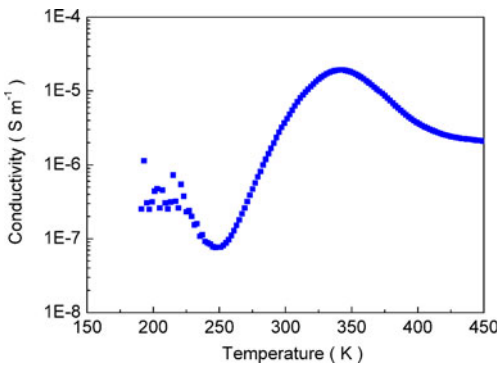

Fig. 5 Temperature dependence of ac-conductivity σ_{ac} of the green body at 100 Hz

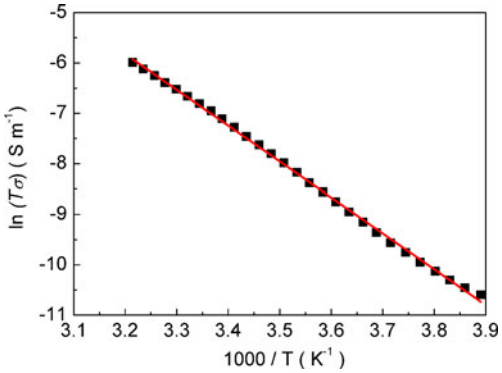

Fig. 6 The value lnσ_{ac} as a function of 1,000/T at 100 Hz for NKN ceramics green body. [The *symbols*: experimental data; the *solid line*: fitting to Eq. (2)]

merge to form conduits or channels for easier transport of ions more or less like normal ion conduction. A mechanism of hopping and transient-fusion and mass exchange would contribute mainly to the percolation process.

After additional one-hour heating at 700 K the green body was cooled to 300 K and no obvious relaxation process was detected (Fig. 7). Furthermore, first to third sequential heating–cooling cycles were carried out, but the relaxation process can be found only first heating. However, the green body presents these relaxation processes again after it is aged 7 days in air; furthermore, the dielectric permittivity is enhanced greatly near percolation threshold (Fig. 7). It is suggested that NKN ceramic green body is very sensitive to humidity and possesses a good reproducibility.

Composites between ferroelectric materials and dispersed conductive phases are of great interest due to a great improvement in dielectric properties for such applications as high capacitance capacitors, non-volatile memory, etc.

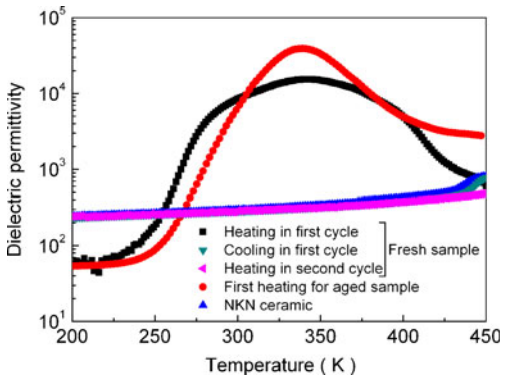

Fig. 7 Temperature dependence of the complex dielectric permittivity real part for fresh and aged nanocrystalline $Na_{0.5}K_{0.5}NbO_3$ ceramic green body with sequential heating–cooling cycles. For sequential heating (2nd and 3rd) sample, the temperature dependences of dielectric permittivity are similar to that of the NKN ceramic. While for cooling processing at different times, dielectric permittivity decreases intensively and is similar to that of the NKN ceramic

Similarly, a giant dielectric material, NKN composite, should be obtained based on percolation theory when water molecules are replaced with conductive particles, such as metal, carbon black, etc. On the other hand, NKN composites or NKN porous ceramics can also be applied as a humidity sensor due to its high sensitivity, good reproducibility, low operation temperature, and relative good chemical and thermal stability.

4 Conclusions

The dielectric spectroscopy of porous NKN ceramic green body presents a complex dielectric relaxation from 200 K to 450 K. It is associated with a complex dynamic characteristic of absorbed water molecules and a percolation effect in the system of water molecule and nanocrystalline NKN particle. A strong dielectric response can be created which results in a reproducible giant dielectric permittivity in NKN green body. These characteristics may suggest some new applications for NKN as giant dielectric composite and humidity sensor.

References

1. B. Jaffe, W.R. Cook Jr., H. Jaffe, *Piezoelectric Ceramics* (Academic, London, 1971)
2. W.W. Wolny, Ceram. Int. **30**, 1079–1083 (2004)
3. Y. Guo, K. Kakimoto, H. Ohsato, Appl. Phys. Lett. **85**, 4121–4123 (2004)
4. M. Matsubara, K. Kikuta, S. Hirano, J. Appl. Phys. **97**, 114105 (2005)
5. M. Matsubara, T. Yamaguchi, W. Sakamoto, K. Kikuta, T. Yogo, S. Hirano, J. Am. Ceram. Soc. **88**, 1190–1196 (2005)
6. M.Z.A. Munshi, *Handbook of Solid State Batteries and Capacitors* (World Scientific Publishing, Singapore, 1995)
7. C.F. Yang, Jpn. J. Appl. Phys. **35**, 1806 (1996)
8. Y. Takeshima, K. Shiratsuyu, H. Takagi, H.Y. Sakabe, Jpn. J. Appl. Phys. **36**, 5870 (1997)
9. S. Kirkpatrick, Rev. Mod. Phys. **45**, 574 (1973)
10. D. Stauffer, Phys. Rep. **54**, 71–74 (1979)
11. T.G. Castner, N.K. Lee, G.S. Cieloszkyk, G.L. Salinger, Phys. Rev. Lett. **34**, 1627 (1975)
12. D.M. Grannan, J.C. Garland, D.B. Tanner, Phys. Rev. Lett. **46**, 375 (1981)
13. D.S. McLachlan, I.I. Oblakova, A.B. Pakhomov, Phys. A **207**, 234 (1994)
14. Y. Song, T.W. Noh, S. Lee, J.R. Gaines, Phys. Rev. B **33**, 904 (1986)
15. C. Pecharromμn, J.S. Moya, Adv. Mater. **12**, 294 (2000)
16. A. Gutina, E. Axelrod, A. Puzenko, E. Rysiakiewicz-Pasek, N. Kozlovich, Y. Feldman, J. Non-Cryst. Solids **235–237**, 302–307 (1998)
17. A. Puzenko, N. Kozlovich, A. Gutina, Y. Feldman, Phys. Rev. B **60**, 14348 (1999)
18. Y. Feldman, A. Puzenko, Y. Ryabov, Phys. Chem. **284**, 139–168 (2002)
19. A. Gutina, E. Rysiakiewicz-Pasek, T. Antropova, Y. Feldman, Microp. Mesop. Mater. **58**, 237–254 (2003)
20. R.K. Chan, D.W. Davidson, E. Whalley, J. Chem. Phys. **43**, 2376 (1965)
21. L. Liu, H. Fan, L. Fang, X. Chen, H. Dammak, M. Pham Thi, Mater. Chem. Phys. **117**, 138–141 (2009)
22. L. Liu, Y. Huang, C. Su, L. Fang, M. Wu, C. Hu, H. Fan, Appl. Phys. A **104**, 1047–1051 (2011)
23. P.B. Macedo, T.A. Litovitz, J. Chem. Phys. **42**, 245 (1965)
24. S.K. Hait, A. Sanyal, S.P. Moulik, J. Phys. Chem. B **106**, 12642 (2002)